PHYSICAL REVIEW B **93**, 195155 (2016)

Quasiparticle band structure of the almost-gapless transition-metal-based Heusler semiconductors

M. Tas,[1,*] E. Şaşıoğlu,[2,†] I. Galanakis,[3,‡] C. Friedrich,[2] and S. Blügel[2]
[1]*Department of Basic Sciences, İstanbul Kemerburgaz University, 34217 İstanbul, Turkey*
[2]*Peter Grünberg Institut and Institute for Advanced Simulation, Forschungszentrum Jülich and JARA, 52425 Jülich, Germany*
[3]*Department of Materials Science, School of Natural Sciences, University of Patras, GR-26504 Patra, Greece*
(Received 15 March 2016; revised manuscript received 5 May 2016; published 25 May 2016)

Transition-metal-based Heusler semiconductors are promising materials for a variety of applications ranging from spintronics to thermoelectricity. Employing the GW approximation within the framework of the FLAPW method, we study the quasiparticle band structure of a number of such compounds being almost gapless semiconductors. We find that in contrast to the sp-electron based semiconductors such as Si and GaAs, in these systems, the many-body corrections have a minimal effect on the electronic band structure and the energy band gap increases by less than 0.2 eV, which makes the starting point density functional theory (DFT) a good approximation for the description of electronic and optical properties of these materials. Furthermore, the band gap can be tuned either by the variation of the lattice parameter or by the substitution of the sp-chemical element.

DOI: 10.1103/PhysRevB.93.195155

I. INTRODUCTION

Gapless materials have been attracting remarkable attention after the discovery of graphene [1] and topological insulators [2] for applications in thermoelectricity, nanoelectronics, spintronics, and optics, due to their high-mobility, robust transport and physical properties [3,4]. They may have either a quadratic energy dispersion like $Hg_{1-x}Cd_xTe$ and $Hg_{1-x}Mn_xTe$ or a linear energy dispersion like graphene and organic salt $\alpha-(BEDT\text{-}TTF)_2I_3$. Materials with linear dispersion obey the relativistic Dirac equation, and thus have very high carrier mobilities. In gapless materials, the charge carriers can easily be excited from the valence band to the conduction band without a cost of energy. Furthermore, one can easily change their band structure by external perturbations like pressure, temperature, chemical composition, electric, and magnetic fields. These innate properties make them desirable for multifunctional tasks. For example, electrons and holes can be fully spin-polarized simultaneously allowing tuneable spin transport in spin-gapless semiconductors (SGSs) [5], which make them ideal spin injectors in spintronic devices.

Transition-metal (TM)-based gapless or almost-gapless semiconductors crystallizing in half and full Heusler structures display rich physics ranging from semimetallic and topological insulator phases to heavy fermionic behavior [6]. For example, specific heat measurements of Heusler-type Fe_2VAl showed that it is a candidate $3d$ heavy-fermion system [7]. Indeed, Guo *et al.* [8] concluded via first-principles calculations that Fe_2VAl is a nonmagnetic semimetal with a narrow pseudogap at the Fermi level. On the other hand, narrow band-gap semiconductors in half-Heusler structure XNiSn (X = Ti, Zr, and Hf) and CoTiSb are promising materials for high-temperature thermoelectric applications with a high figure of merit [9–11].

Widely spread standard first-principles calculations addressing the electronic and optical properties of solid compounds including also the TM-based gapless and almost-gapless (also known as zero or small band-gap, respectively) semiconductors (SCs) are based on density-functional theory (DFT) within either the local-density approximation (LDA) or the generalized gradient approximation (GGA) to the exchange-correlation functional [8,12–14]. As it is known, DFT is restricted to the calculation of ground-state properties, and it fails in describing the band gap and properties that rely on excited states. The deficiency of DFT for materials from weak to intermediate correlations can be healed by the GW approximation, which is shown to be quite successful in describing the excited states, i.e., the band gaps and optical properties [15].

Gapless or almost-gapless semiconductors are crucial for thermoelectric applications since such materials present a high figure of merit. To this respect, the so-called semi- (or half-) Heusler compounds with 18 valence electrons like CoTiSb or NiTiSn have been widely studied (for a review, see Ref. [16]). On the other hand, full-Heusler compounds [17–19] constitute a much larger reservoir to identify and study semiconducting materials suitable for thermoelectric applications. According to the Slater-Pauling rule, full-Heusler compounds with 24 valence electrons can be expected to be either magnetic or non-magnetic semiconductors [17–19]. Small-gap 24-valence-electron semiconductors are most likely to be found among the quaternary Heuslers due to the existence of three different TM atoms in the unit cell [19].

The aim of the present work is a systematic study of the electronic structure of the TM-based SCs [$(XX')YZ$, where X, X′, and Y are TM elements, and Z is an sp element] with almost zero band gaps. Due to the presence of the TMs with narrow d bands the correlation effects are expected to play a dominant role in electronic structure of these materials. Using the GW approximation within the framework of the full potential linearized augmented plane-wave (FLAPW) method, we show that in contrast to sp-electron based SCs such as Si and GaAs, in these systems the many-body correlations have a minimal effect on the electronic band structure. We find that for many compounds the change of the band gap is less than 0.2 eV, which makes the starting point DFT-LDA (DFT-GGA) a good

*murat.tas@kemerburgaz.edu.tr
†e.sasioglu@gmail.com
‡galanakis@upatras.gr

approximation for the description of electronic and optical properties of these materials. Moreover, it is demonstrated that the band gap can be tuned either by the substitution of the Z element or by a variation of the lattice parameter. The rest of the paper is organized as follows. In Sec. II, we briefly describe the computational scheme. Section III presents the computational results and discussion. In Sec. IV, we give the conclusions.

II. COMPUTATIONAL METHOD

The ground-state calculations are carried out using the FLAPW method as implemented in the FLEUR code [20] within the generalized gradient approximation (GGA) of the exchange-correlation potential as parameterized by Perdew, Burke, and Ernzerhof (PBE) [21]. For all calculations, we use angular momentum and plane-wave cutoff parameters of $l_{\max} = 8$ inside the spheres and $k_{\max} = 4$ bohr^{-1} for the outside region. The DFT-PBE calculations are performed using a $16 \times 16 \times 16$ **k**-point grid. In order to accurately describe the unoccupied states we use local orbitals. Note that in the case of (CoCr)TiBi local orbitals are also used for semi-core $5d$ states of bismuth.

We performed the one-shot GW calculations using the SPEX code [22]. In the one-shot GW approach off-diagonal elements in the self-energy operator $\Sigma_\sigma(E_{n\mathbf{k}\sigma})$ are ignored and corresponding expectation values of the local exchange-correlation potential V_σ^{XC} are subtracted in order to prevent double counting. Within this framework, the Kohn-Sham (KS) single-particle wave functions $\varphi_{n\mathbf{k}\sigma}^{\mathrm{KS}}$ are taken as approximations to the quasiparticle (QP) wave functions. Hence the QP energies $E_{n\mathbf{k}\sigma}$ are calculated as a first-order perturbation correction to the KS values $E_{n\mathbf{k}\sigma}^{\mathrm{KS}}$ as [23]

$$E_{n\mathbf{k}\sigma} = E_{n\mathbf{k}\sigma}^{\mathrm{KS}} + \langle \varphi_{n\mathbf{k}\sigma}^{\mathrm{KS}} | \Sigma_\sigma(E_{n\mathbf{k}\sigma}) - V_\sigma^{\mathrm{XC}} | \varphi_{n\mathbf{k}\sigma}^{\mathrm{KS}} \rangle, \qquad (1)$$

where n, $\mathbf{k}$, and σ are band index, Bloch vector, and electron spin, respectively.

The dynamically screened Coulomb interaction W is expanded in the mixed product basis set having contributions from the local atom-centered muffin-tin spheres, and plane waves in the interstitial region [24]. For the mixed product basis set we used the cutoff parameters $L_{\max} = 4$ and $G_{\max} = 3$ Bohr^{-1}. For each compound, three different **k**-point grids are used to sample the full Brillouin zone: $4 \times 4 \times 4$, $6 \times 6 \times 6$, and $8 \times 8 \times 8$. The relativistic corrections are treated at the scalar-relativistic level (no spin-orbit coupling) for valence states, while the full Dirac equation is employed for the core states. We have converged the excitation energies with the number of unoccupied states and observed that with 300 bands the band gap is converged to within less than 10 meV for all compounds under study.

The considered TM-based SCs crystallize in the LiMgPdSn-type crystal structure with the space group of $F\bar{4}3m$. They are made up of four interpenetrating face-centered cubic (fcc) lattices. The crystal structure is described by the chemical formula (XX′)YZ, where X, X′, and Y are TMs, and Z is an sp element. The atoms are placed at four equidistant sites on the diagonal of the fcc lattice in sequence of X-Y-X′-Z. The valence of the TMs follows the same order as in their chemical formula, i.e., X atoms have the highest valence, while Y atoms have the lowest.

To identify TM-based gapless or almost-gapless SCs, we use the well-known Slater-Pauling (SP) rule [17,25], which relates the total spin magnetic moment per unit cell in μ_{B} (M_t) of compounds to their total number of valence electrons (N_v). For the LiMnPdSn-type quaternary compounds, the SP rule takes the form $M_t = N_v - 24$ [19] and thus potential zero-gap SCs should have 24 valence electrons per formula unit. We have chosen as candidates the (FeMn)TiP, (CoMn)TiSi, (CoMn)VAl, (CoFe)TiAl, (CoCr)TiP, (CoCr)TiAs, (CoCr)TiSb, and (CoCr)TiBi compounds. Since $N_v = 24$, the SP rule states that their total spin magnetic moment should be zero.

III. RESULTS AND DISCUSSION

A. DFT results

We begin our discussion with the results obtained from the standard GGA formalism of DFT. Since the compounds under study do not exist experimentally, we have first determined the equilibrium lattice constants using total energy calculations and fitting the standard equation of state to the total energy curve. Note that full-Heuslers including also the quaternary Heuslers is a class of materials where most of the compounds have been first studied by simulations and then have been grown experimentally [6], and thus one should envisage that the growth of the compounds of the present study is feasible. The obtained results are presented in the first column of Table I. Lattice constants present large variations from 5.64 Å for (FeMn)TiP to 6.26 Å for (CoCr)TiBi due to the large atomic radius of the Bi atoms. Interestingly, these values are similar to the lattice constants of existing binary semiconductors.

In the case of Heusler compounds with 24 valence electrons, the ground state can be either nonmagnetic semiconducting or fully compensated ferrimagnetic semiconducting [19]; in the latter case, the atoms possess finite atomic spin magnetic moments but the total magnetization is zero. Our first-principles calculations reveal that for the compounds under study, the nonmagnetic semiconducting phase is the ground state since we were not able to converge to a fully compensated ferrimagnetic state irrespectively of the initial configuration of the atomic spin magnetic moments considered in our calculations.

B. Band structure and energy gaps

Using the DFT results as an input we performed one-shot GW calculations. Using (CoFe)TiAl as a representative example we will discuss the changes in the band structure. The situation is similar for the other compounds. First, we should establish the convergence of the energy gap using GW with respect to the number of **k** points and the number of energy bands taken into account in the calculation. We present the results of our convergence tests in Fig. 1. With a specific **k**-point grid we need around 300 empty bands to have reliable values for the GW energy gaps which corresponds to about 75 empty bands per atom since there are four atoms per unit cell, a value which is similar to the well-known semiconductors like Si or Ge. As the grid becomes denser the energy gaps

TABLE I. Calculated equilibrium lattice constants a (in angstroms), PBE and GW band gaps, and transition energies (in eV) between certain high-symmetry points for TM-based SCs.

				PBE			GW		
Compound	a (Å)	E_g^{PBE} (eV)	E_g^{GW} (eV)	$\Gamma \to \Gamma$	$\Gamma \to X$	$X \to X$	$\Gamma \to \Gamma$	$\Gamma \to X$	$X \to X$
(FeMn)TiP	5.64	0.46	0.60	0.66	0.46	0.53	0.76	0.66	0.60
(CoMn)TiSi	5.73	0.31	0.50	0.31	0.32	0.59	0.52	0.50	0.61
(CoMn)VAl	5.74	−0.07	−0.15	0.18	−0.07	0.25	0.26	−0.15	0.02
(CoFe)TiAl	5.81	0.08	0.30	0.08	0.12	0.45	0.30	0.33	1.08
(CoCr)TiP	5.72	0.23	0.34	0.54	0.23	0.28	0.71	0.41	0.34
(CoCr)TiAs	5.87	0.09	0.16	0.35	0.09	0.28	0.16	0.26	0.33
(CoCr)TiSb	6.10	−0.01	0.13	0.30	−0.01	0.28	0.41	0.13	0.30
(CoCr)TiBi	6.26	−0.17	−0.04	0.07	−0.17	0.29	−0.29	−0.04	0.29

become smaller but we can see that the difference between the $6 \times 6 \times 6$ and $8 \times 8 \times 8$ is of the order of 0.01–0.02 eV and thus the former can be safely used.

We present the calculated band structure in Fig. 2 using both the PBE parametrization of GGA and the GW method. First, we shortly analyze the character of the bands at the Γ point, giving the character of the orbitals in real space. The arguments are similar to the case of usual half-metallic full and ordered quaternary Heusler compounds [17,19]. There is an s-band low in energy not shown in Fig. 1. The lowest shown bands are the Al p bands, which are triple-degenerate at the Γ point and which also accommodate the d charge of the transition metal atoms. Then there are the double-degenerate e_g and triple-degenerate (at the Γ point) t_{2g} d hybrids of the TM atoms, which are in tetrahedral symmetry. The states just below and just above the Fermi level are the triple-degenerate t_{1u} and the double-degenerate e_u states which are located exclusively at the Co and Fe sites in octahedral symmetry; for an extensive discussion see Refs. [17,19].

The GW band structure presented in Fig. 2 looks qualitatively similar to the PBE-GGA results. The bands, however, differ quantitatively especially at energies away from the Fermi energy where the p and the bonding e_g and t_{2g} hybrids reside. The change in the bands originating from the e_u and t_{1u} hybrids is much smaller and less visible. Mainly the GW quasiparticle corrections push the conduction (e_u hybrids) and valence (t_{1u} hybrids) bands, respectively, up and down, hence opening the band gap, but the broadening does not exceed 0.2 eV. As a result within PBE-GGA, (CoFe)TiAl is an almost-gapless semiconductor with a direct gap at the Γ point of 0.08 eV, while within GW, one could classify it as a narrow-band semiconductor with a direct energy gap of 0.30 eV.

Finally, in Table I, we present both the PBE-GGA and GW energy gaps for all compounds under study. First, we should note that, for any chosen **k** point, the bands are well separated by a finite energy gap. This is reflected in the direct $\Gamma \to \Gamma$ and $X \to X$ energy band gaps presented in the table. For many of the compounds under study, the fundamental energy gaps (E_g^{PBE} and E_g^{GW}) correspond to the indirect $\Gamma \to X$ gaps as seen in Table I. Moreover, in the case of (CoMn)VAl, (CoCr)TiSb, and (CoCr)TiBi, the overlap of the valence and conduction bands is such that instead of getting a semiconductor we get a semimetallic-like behavior of the density of states, i.e., in this case the bottom of the conduction band is lower in energy than the top of the valence band. This behavior is reflected in the negative values given in the table.

The size of the gaps increases with the valence of the sp atom as we move from Al to Si and then to P where the valence electrons increase by one. A similar remark can be made when we move along a column of isovalent chemical

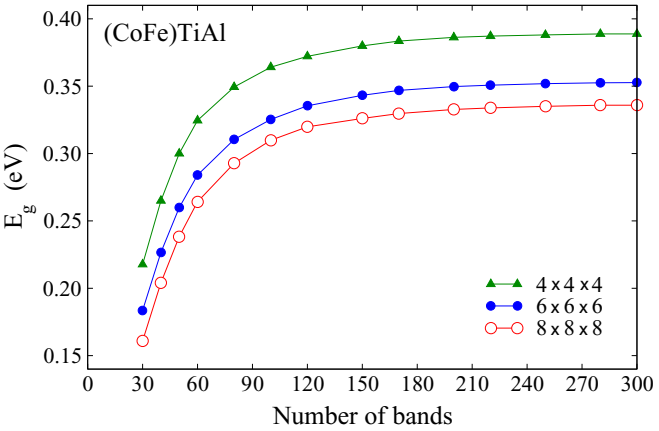

FIG. 1. Convergence of the energy band gap with the number of bands and the **k**-point grid for (CoFe)TiAl.

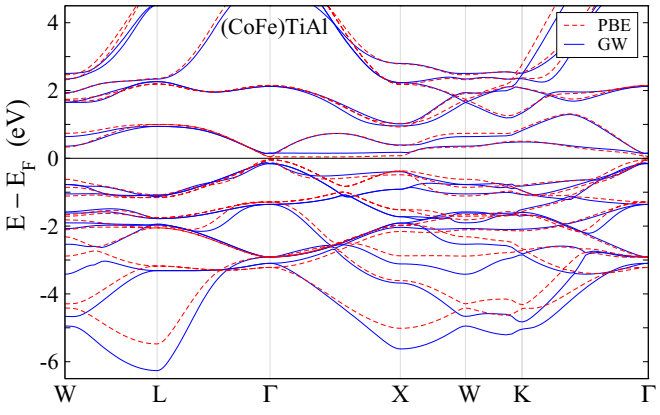

FIG. 2. Calculated electronic band structure of (CoFe)TiAl along the high-symmetry directions in the first Brillouin zone using either the PBE-GGA (red dashed line) or the GW (blue solid line) approximations.

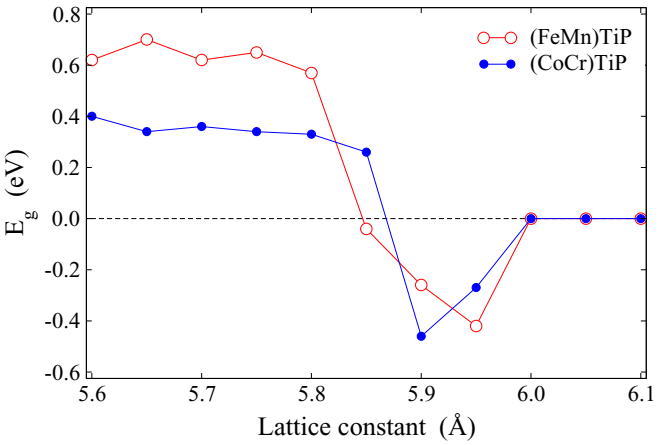

FIG. 3. Energy band-gap tuning with the variation of the lattice parameter for the compounds (FeMn)TiP and (CoCr)TiP using the GW approximation.

elements from the lighter P to As, Sb and finally Bi. To understand this trend, we have to remark that the d hybrids below the Fermi level have also a small portion of p character. For lighter element like Al, this admixture is sizeable and contributes to the opening of the gap similarly to the usual $p-d$ hybridization scheme in semiconductors [12]. As Al is substituted by heavier atoms, their p states are located deeper in energy, the admixture of the p character in the d bands decreases and the energy gap shrinks. The use of the GW self-energy increases systematically the values of both direct and indirect bands gaps but this increase does not exceed 0.2 eV in any of the cases. Even this moderate increase can transform the character of (CoCr)TiSb from semimetallic-like to semiconducting.

Finally, we should also discuss the applicability of GW to the study of the electronic band structure of materials. Although, in principle, GW is a more elaborate method to study the band structure of solids since it includes the quasiparticle corrections, its success with respect to standard density-functional calculations is not guaranteed and results should be confirmed by experiments. Recently, Meinert *et al.* [15] studied the band structure of the half-metallic ferromagnetic full Heusler compounds Co_2MnSi and Co_2FeSi via one-shot GW calculations and found that the many-body corrections are crucial especially for the latter system, and experimentally studied spectra of both materials are well described by the GW calculations. In contrast, the band gap of wurtzite ZnO is repeatedly underestimated by more than 1 eV within the GW calculations with respect to its experimental value. A recent GW calculation with the FLAPW method has found its band gap higher than previous studies but still lower than its measured value [26]. Better agreement with experiment can be achieved with a self-consistent procedure [27]. Similarly, in the case of FeS_2 pyrite the one-shot GW calculations find a lower value for the fundamental band gap [28].

C. Effect of the lattice parameter

Expanding or compressing lattices, and even slight changes in the chemical composition alter dramatically the lattice constants of compounds and their band-gap energies. This so-called band-gap tuning or band-gap engineering has become quite important in designing new multifunctional devices. The GW band-gap energies of the compounds (FeMn)TiP and (CoCr)TiP are plotted as a function of their lattice constant in Fig. 3. (FeMn)TiP is found to be a SC in both PBE and GW calculations at its equilibrium lattice constant of 5.64 Å (see Table I), but it is predicted to be a semimetal when its lattice constant is increased just about 3.6%. Similarly, (CoCr)TiP seems to make a sharp transition from a semiconducting to a semimetallic phase when its lattice constant is extended approximately 2.3% from its equilibrium value. Both compounds are found to be gapless when their lattice constants are assumed to be 6 Å. Tailoring of the band-gap energy by substitution of sp elements in compounds (CoCr)TiZ is already discussed above.

IV. CONCLUSIONS

We have studied the quasiparticle band structure of several TM-based almost-gapless Heusler semiconductors (XX′)YZ by using the one-shot GW approximation within the framework of the FLAPW method. We find that in contrast to sp-electron based semiconductors such as Si and GaAs, in these systems the many-body correlations have a minimal effect on the electronic band structure. For these compounds, the change of the energy band gap is less than 0.2 eV. Thus the standard density-functional-theory based first-principles calculations are a good approximation for describing the electronic properties of these materials. Furthermore, the band gap of these compounds can be tuned by varying the lattice parameter or by substituting the main group sp element.

ACKNOWLEDGMENTS

M. Tas acknowledges kind hospitality of the Peter Grünberg Institut and Institute for Advanced Simulation, Forschungszentrum Jülich, Germany.

[1] K. S. Novoselov, A. K. Geim, S. V. Morozov, D. Jiang, Y. Zhang, S. V. Dubonos, I. V. Grigorieva, and A. A. Firsov, Science **306**, 666 (2004).

[2] M. Z. Hasan and C. L. Kane, Rev. Mod. Phys. **82**, 3045 (2010).

[3] I. M. Tsidilkovski, *Electron Spectrum of Gapless Semiconductors*, edited by K. von Klitzing, Springer Series in Solid-State Sciences Vol. 116 (Springer-Verlag, Berlin, 1997).

[4] X. Wang, S. X. Dou, and C. Zhang, NPG Asia Mater. **2**, 31 (2010); and references therein.

[5] X. L. Wang, Phys. Rev. Lett. **100**, 156404 (2008); X. Wang, G. Peleckis, C. Zhang, H. Kimura, and S. Dou, Adv. Mater. **21**, 2196 (2009).

[6] T. Graf, C. Felser, and S. S. P. Parkin, Prog. Solid State Chem. **39**, 1 (2011).

[7] Y. Nishino, M. Kato, S. Asano, K. Soda, M. Hayasaki, and U. Mizutani, Phys. Rev. Lett. **79**, 1909 (1997).
[8] G. Y. Guo, G. A. Botton, and Y. Nishino, J. Phys. Condens. Matter **10**, L119 (1998).
[9] T. Jaeger, C. Mix, M. Schwall, X. Kozina, J. Barth, B. Balke, M. Finsterbusch, Y. U. Idzerda, C. Felser, and G. Jakob, Thin Solid Films **520**, 1010 (2011).
[10] J.-W. G. Bos and R. A. Downie, J. Phys. Condens. Matter **26**, 433201 (2014).
[11] E. Rausch, S. Ouardi, U. Burkhardt, and C. Felser, arXiv:1502.03336.
[12] M. Weinert and R. E. Watson, Phys. Rev. B **58**, 9732 (1998).
[13] K. Sato and H. Katayama-Yoshida, Semicond. Sci. Technol. **17**, 367 (2002).
[14] C. G. Van de Walle and J. Neugebauer, J. Appl. Phys. **95**, 3851 (2004).
[15] M. Meinert, C. Friedrich, G. Reiss, and S. Blügel, Phys. Rev. B **86**, 245115 (2012).
[16] S. Chen and Z. Ren, Mater. Today **16**, 387 (2013).
[17] I. Galanakis, P. H. Dederichs, and N. Papanikolaou, Phys. Rev. B **66**, 174429 (2002).
[18] S. Skaftouros, K. Özdoğan, E. Şaşıoğlu, and I. Galanakis, Phys. Rev. B **87**, 024420 (2013).
[19] K. Özdoğan, E. Şaşıoğlu, and I. Galanakis, J. Appl. Phys. **113**, 193903 (2013).
[20] www.flapw.de
[21] J. P. Perdew, K. Burke, and M. Ernzerhof, Phys. Rev. Lett. **77**, 3865 (1996).
[22] C. Friedrich, S. Blügel, and A. Schindlmayr, Phys. Rev. B **81**, 125102 (2010).
[23] I. Aguilera, C. Friedrich, G. Bihlmayer, and S. Blügel, Phys. Rev. B **88**, 045206 (2013).
[24] T. Kotani and M. van Schilfgaarde, Solid State Commun. **121**, 461 (2002).
[25] J. C. Slater, Phys. Rev. **49**, 537 (1936); L. Pauling, *ibid.* **54**, 899 (1938).
[26] C. Friedrich, M. C. Müller, and S. Blügel, Phys. Rev. B **83**, 081101(R) (2011); and references therein.
[27] J. Klimes, M. Kaltak, and G. Kresse, Phys. Rev. B **90**, 075125 (2014).
[28] T. Schena, G. Bihlmayer, and S. Blügel, Phys. Rev. B **88**, 235203 (2013).